

Research Article

Research on Polymer Viscous Flow Activation Energy and Non-Newtonian Index Model Based on Feature Size

Yan Lou , Qunan Lei, and Gang Wu

College of Mechatronics and Control Engineering, Shenzhen University, Shenzhen, Guangdong, China

Correspondence should be addressed to Yan Lou; susanlou121@163.com

Received 17 March 2019; Accepted 9 April 2019; Published 2 May 2019

Academic Editor: Alexandra Muñoz-Bonilla

Copyright © 2019 Yan Lou et al. This is an open access article distributed under the Creative Commons Attribution License, which permits unrestricted use, distribution, and reproduction in any medium, provided the original work is properly cited.

The viscous flow activation energy and non-Newtonian index properties of polymer based on feature size were studied through a series of experiments on the rheological properties of amorphous polymer polymethyl methacrylate (PMMA), semi-crystalline polymer polypropylene (PP), and crystalline polymer high-density polyethylene (HDPE) using capillary die with hole diameters of $\varphi 0.3$ mm, $\varphi 0.5$ mm, $\varphi 1.0$ mm, and $\varphi 2.0$ mm. The results show that the viscous flow activation energy of PMMA decreases with the feature size under microscopic scale. And the viscous flow activation energy of PP and HDPE increases with hole diameters of the die. Under macroscopic scale, the difference in viscous flow activation energy of all polymer materials is significantly reduced with hole diameters of the die. For the non-Newtonian index of the three polymer materials, it decreases with the feature size under the microscopic scale while it increases or does not change with the feature size under the macroscopic scale. At the same time, for different high polymer materials, the viscous flow activation energy model (SVAE model) and non-Newtonian index model (SNNE model) based on feature size were established. Finally, the accuracy and effectiveness of the SVAE model and the SNNE model are verified by comparing with the traditional model and reference data. The viscous flow activation energy and non-Newtonian index values of the polymer material can be calculated conveniently and accurately.

1. Introduction

At present, most studies on rheological properties of polymers are biased towards the viscosity characteristics of materials and the establishment of viscosity models [1, 2], while the research and modeling on viscous flow activation energy and non-Newtonian properties of polymer melts are few. It is well known that for most polymers viscous flow activation energy is the minimum energy required for the flow unit (chain segment) to overcome the barrier and transit from the in-situ position to the nearby “hole” in the flow process, and it is a sign of the sensitivity for the apparent shear viscosity to temperature. Therefore, the viscous flow activation energy can be used to judge the degree of difficulty on the material flow and evaluate its processing performance. In addition, the sensitivity of the melt shear viscosity to the shear rate is described by the non-Newtonian index because the polymer fluid is mostly pseudoplastic non-Newtonian fluid, and the smaller non-Newtonian index value suggests

the stronger both non-Newtonian and the sensitivity of the shear viscosity to the shear rate [3].

Some scholars have conducted preliminary research on viscous activation energy and non-Newtonian index. E. A. Collins et al. [4] studied the rheological properties of a series of polyvinyl chloride (PVC) resins. They found that the viscous flow activation energy of the melt is not constant and has different values at low and high temperatures. The activation energy can be independent on the type of polymer. S. Nair et al. [5–7] obtained the kinetic and shear thickening mechanism based on mixture viscous flow activation energy changes through the experiment of the rheological properties of mixed polymer melt. By studying the macroscopic deformation rheological properties of the composite at a series of hole diameters of the die ($\varphi 8$ – $\varphi 36$ mm), K. Hamad et al. [8–11] found that the viscous flow activation energy decreases with the shear rate. M. Kaseem [12–14] studied the rheological properties of polymer composites at the die with hole diameter of $\varphi 0.5$ – $\varphi 4$ mm and found that the viscous flow

TABLE 1: Pretreatment and experimental parameters of the three materials.

| Material | Manufacturer | Brand | Drying temperature/ $^{\circ}\text{C}$ | Drying time/h | Shear rate/ s^{-1} | Testing temperature |
|----------|--------------|--------|--|---------------|-----------------------------|---------------------------------------|
| PMMA | LG | CM205 | 90 | 5 | $3\sim 10^4$ | 210, 230, 250, 270 $^{\circ}\text{C}$ |
| PP | LOTTE | J560s | Not absorbing | 0 | $3\sim 10^4$ | 200, 220, 240, 280 $^{\circ}\text{C}$ |
| HDPE | LG | ME9180 | Not absorbing | 0 | $3\sim 10^4$ | 200, 220, 240, 260 $^{\circ}\text{C}$ |

activation energy of the melt decreases with hole diameters of the die and that the non-Newtonian index increases with hole diameters of the die. However, the corresponding mathematical model was not established.

Minjie Wang et al. [15–18] tested the melt shear viscosity of polymers at the die with different hole diameters of $\phi 0.5$, $\phi 1$, and $\phi 1.5\text{mm}$ and analyzed both law of viscous flow activation energy and non-Newtonian index of polymer melt using hole diameters of $\phi 0.5\text{mm}$ under varied shear rate and temperature. But the influence of different hole diameters on both viscous flow activation energy and non-Newtonian index was not analyzed. Chongzhou Z. Wu [19] processed the melt rheological data of low-density polyethylene at the die with hole diameter of $\phi 0.56\text{mm}$ using orthogonal polynomial regression analysis and obtained a non-Newtonian index model without considering the influence of feature size.

In summary, whether it is the rheological properties of pure polymer or that of composite polymer, it involves both melt viscous flow activation energy and the non-Newtonian index. It has a significant influence on the rheological properties, but at present there is no systematic study including mathematical model on both viscous flow activation energy and non-Newtonian index based on the feature size.

Therefore, three materials were used in research; those are amorphous polymer polymethyl methacrylate (PMMA), semi-crystalline polymer polypropylene (PP), and crystalline polymer high-density polyethylene (HDPE). These three polymers are widely used as polymer materials, and they represent three states of high polymer, namely, amorphous, semi-crystalline, and crystalline. The melt rheology analysis was performed using a single barrel capillary rheometer.

The hole diameter of the die is $\phi 0.3 \sim 2\text{mm}$, covering the macroscopic and microscopic scales. The compression bar rate is $0.0139 \sim 2.0833\text{mm/s}$ (the corresponding shear rate is $3 \sim 10^4 \text{ s}^{-1}$). Based on the rheological shear viscosity test of melts on different polymer materials with different die diameters, both viscous flow activation energy and non-Newtonian index mathematical models based on feature size were established, and their error analysis were carried out. It provides a novel method to predict the viscous flow activation energy and the non-Newtonian index of the polymer melt.

2. Experiment

The experimental materials were selected from optical grade polymethyl methacrylate (PMMA), polypropylene (PP), and

high-density polyethylene (HDPE). The experimental equipment is a capillary rheometer (Gottfert, Germany, RG20 type), and the hole diameter of the die includes both microscales ($\phi 0.3\text{mm}$ and $\phi 0.5\text{mm}$) and macroscales ($\phi 1\text{mm}$ and $\phi 2\text{mm}$). To focus on the effect of the die hole diameter on the viscous flow activation energy and the non-Newtonian index, the length diameter ratios of the dies are all of the same value of 10. Exactly, the length-diameter ratios of the dies are 3-0.3mm, 5-0.5mm, 10-1mm, and 20-2mm, respectively. The pretreatment and experimental parameters of the three materials are shown in Table 1.

In order to study the rheological properties of polymer at the microscopic and macroscopic dimensions, the rheology experiments were conducted at different shear rates and different hole diameters of the die based on the above materials. The polymer melting time was 500 s. The data points were collected at a shear rate ranging from 3 to 10^4 s^{-1} to obtain the shear viscosity and shear stress values of the polymer melt. Three replicates were performed under each group of parameters to obtain the experimental data.

3. Results and Discussion

3.1. Analysis of Rheological Properties of Polymer Melt

3.1.1. Analysis of Viscous Flow Activation Energy. The shear viscosity data of different hole diameters of the die were obtained by melt rheology experiments. The relationship between the apparent shear viscosity of the polymer and the temperature is in accordance with the Arrhenius empirical formula [4]:

$$\eta_a = Ae^{E_\eta/RT} \quad (1)$$

where η_a is apparent shear viscosity, $\text{Pa} \cdot \text{s}$. A is a constant, E_η is the viscous flow activation energy, kJ/mol . R is gas constant, and $8.314 \text{ J}/(\text{mol} \cdot \text{K})$. T is absolute temperature, K .

Deduced by taking the logarithm of the above formula, we can get $\ln \eta_a = (E_\eta/R)(1/T) + \ln A$. The curve of the melt shear viscosity of the three materials with temperature is obtained by the $\ln \eta_a - 1/T$ curve. The slope of the viscosity curve of each material, $k = E_\eta/R$, is taken to obtain the viscous flow activation of the polymer melt at different hole diameters of the die and shear rates. Figure 1 shows the curve of viscous flow activation energy to shear rate for three materials at different hole diameters of the die. D means the hole diameter of die, and $\dot{\gamma}$ means the shear rate.

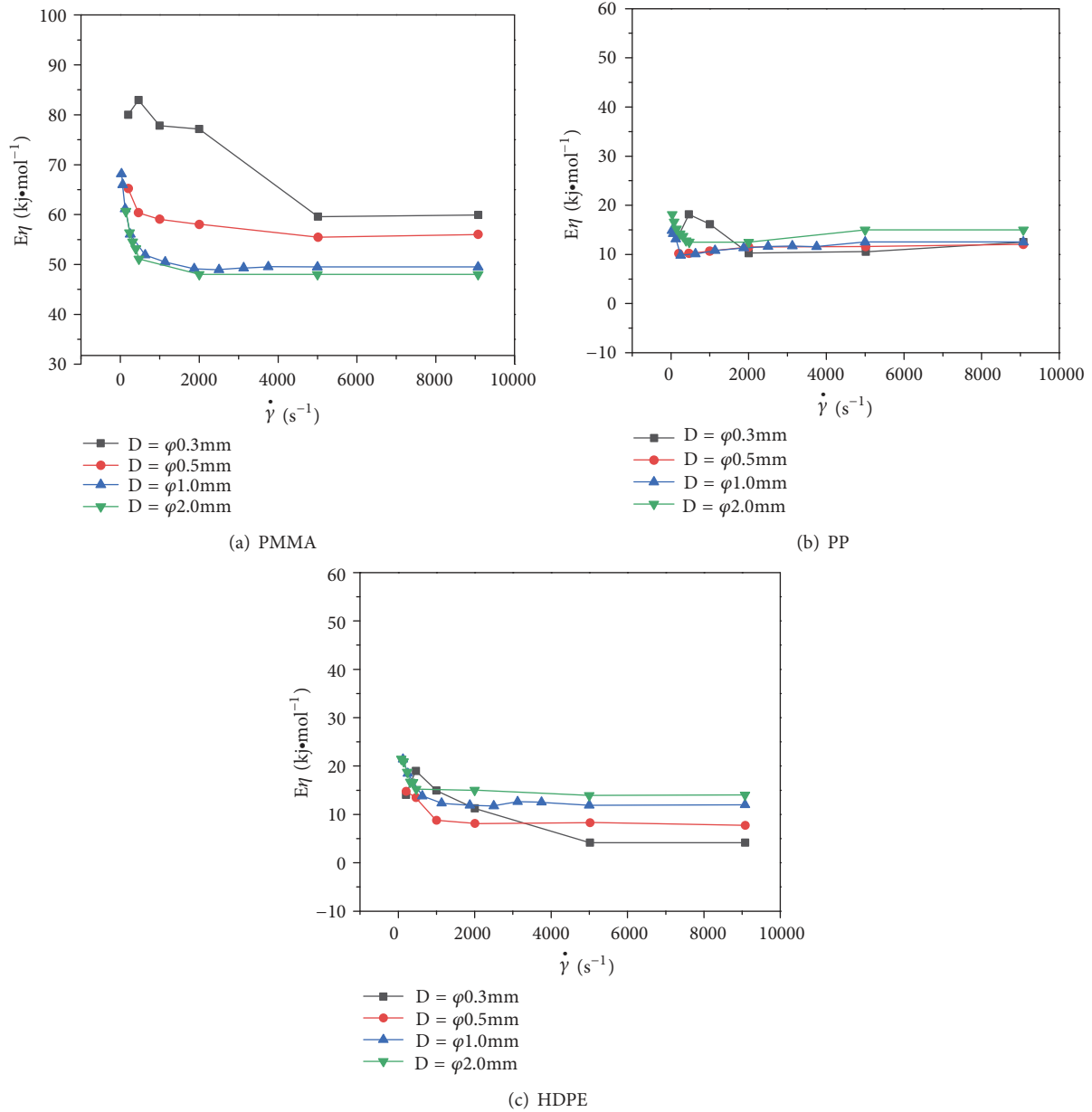


FIGURE 1: Curve of viscous flow activation energy to shear rate for three materials at different hole diameters of the die. (a) PMMA; (b) PP; (c) HDPE.

It can be seen that the viscous flow activation energy of the three materials decreases with the shear rate at low shear rates and keeps constant at high shear rates, which indicates that the sensitivity of the viscosity to temperature reduces with the shear rate at low shear rate while keeping constant at high shear rate.

At very low shear rates of less than 460 s^{-1} , the viscous flow activation energy is affected by both wall slip and microscopic viscosity. When the hole diameter of the die is $\varphi 0.3 \text{ mm}$, the resistance-increase effect of wall slip on melt flow is dominant. With the increased shear rate, the resistance-increase effect increases, so the viscous flow activation energy is larger. When the hole diameter of the die is larger than $\varphi 0.5$

mm , the microscopic viscosity has a major influence on the melt flow, and it is reduced with the shear rate. Therefore, the viscous flow activation energy decreases with the shear rate. When the shear rate is larger than 460 s^{-1} , the microscopic viscosity has also a major influence, so the viscous flow activation energy of the three materials decreases with the shear rate. However, at high shear rates (larger than 1000 s^{-1}), the effect of microscopic viscosity is negligible and mainly is affected by wall slip, so the viscous flow activation energy keeps constant with the shear rate. When the hole diameter of the die is larger than $\varphi 1.0 \text{ mm}$ at high shear rate, the viscosity and the wall slip are both negligible. This result is basically consistent with what were obtained in the literatures [20, 21].

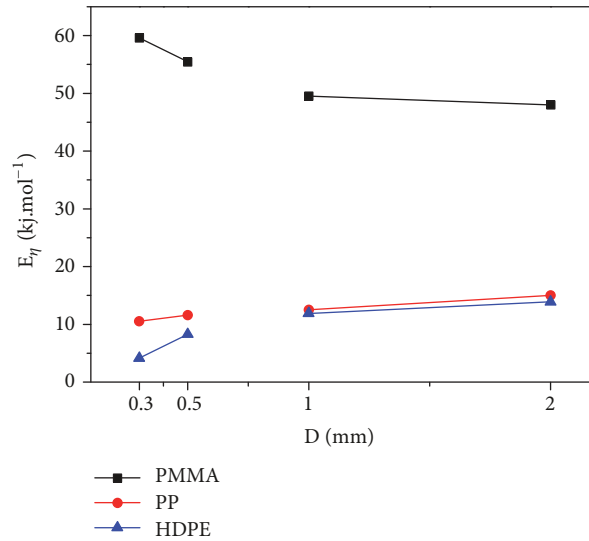


FIGURE 2: Viscous flow activation energy at both microscales and macroscales with the shear rate of 5000 s^{-1} .

It was also found that the viscous flow activation energy of PMMA decreased significantly with hole diameter of $\varphi 0.3\text{mm}$ and $\varphi 0.5\text{mm}$ at the shear rate of 5000 s^{-1} as shown in Figure 2. It indicates that there is a resistance-increasing effect on the melt flow for PMMA due to the existence of wall slip at the microscopic scale. The smaller the hole diameter of the die, the more obvious the resistance-increasing effect [22]. The deformation energy storage and dissipation are increased, so the viscous flow activation energy is increased [23]. It is consistent with the findings of J. Z. Liang [13], who reported that the deformation energy storage and dissipation decrease with the microchannel diameter. At the macroscopic scale (die diameter is $\varphi 1.0\text{mm}$ and $\varphi 2.0\text{mm}$), the effect of wall slip on the melt flow is eliminated. And the difference of the viscous flow activation energy on the PMMA is significantly reduced.

For the crystalline polymer PP and HDPE, at the microscopic scale (hole diameter of the die is $\varphi 0.3\text{mm}$ and $\varphi 0.5\text{mm}$), the viscous flow activation energy increases with the die diameter, which is exactly the opposite of the PMMA law as shown in Figure 2. The wall slip has a resistance-reducing effect on PP and HDPE materials. The smaller the hole diameter of the die, the more obvious the resistance-reducing effect [22]. The flow deformation energy storage and dissipation are reduced, so the viscous flow activation energy is reduced. Also, the effects of wall slip are eliminated at macroscopic dimensions ($\varphi 1 \text{ mm}$ and $\varphi 2 \text{ mm}$), so the difference of viscous flow activation energy on PP and HDPE melts is significantly reduced.

It also can be seen from Figure 2 that the noncrystalline PMMA has the highest viscous flow activation energy due to the molecular chain structure. There are two side groups for PMMA, namely, $-\text{CH}_3$ side methyl group and $-\text{COOCH}_3$ side acetate group, which makes its molecular chain hard, leading to a higher viscous flow activation energy than that of both PP and HDPE. PP molecular chain structure only contains a side methyl group, $-\text{CH}_3$, so the viscous flow activation

energy is second. While the molecular backbone structure of HDPE does not contain any side groups, and only few short branches, the molecular chain is more flexible. The internal rotation is easy to carry out, and the motion unit has a small chain segment, so the viscous flow activation energy is the lowest [24]. Therefore, in addition to the melt shear rate, the die diameter and molecular chain structure have a significant influence on the viscous flow activation energy.

3.1.2. Analysis of Non-Newtonian Index. Since the polymer materials in this test are all pseudoplastic non-Newtonian fluids, the shear stress and shear rate are in accordance with the power law function equation [12]: $\tau = K\dot{\gamma}^n$. Taking the logarithm on the two sides of the equation as follows:

$$\lg\tau = \lg K + n \lg \dot{\gamma} \quad (2)$$

where τ is shear stress, K is consistency coefficient, n is non-Newtonian index, and $\dot{\gamma}$ is shear rate.

To focus on studying the effect of hole diameter of the die on the non-Newtonian index, the shear rate of $10^3 \sim 10^4 \text{ s}^{-1}$ is considered because at the shear rate of $10^3 \sim 10^4 \text{ s}^{-1}$ the non-Newtonian index of the polymer melt is little affected by the shear rate [25]. The calculation of the non-Newtonian index considers the influence of both temperature and hole diameter of the die instead of the shear rate [13, 26]. After linear regression of the curves, the non-Newtonian index of each polymer melt at both microscales and macroscales was obtained at different temperatures as shown in Figure 3.

It can be seen from Figure 3 that the non-Newtonian index of the three materials increases with temperature regardless of the amorphous or crystalline polymer, which indicates that the sensitivity of the viscosity to the shear rate decreases with temperature. It is due to the fact that the higher the temperature, the more intense the segment movement. The entanglement of the chain is solved by the shear stress; meanwhile, the reestablishment of that is obtained by the

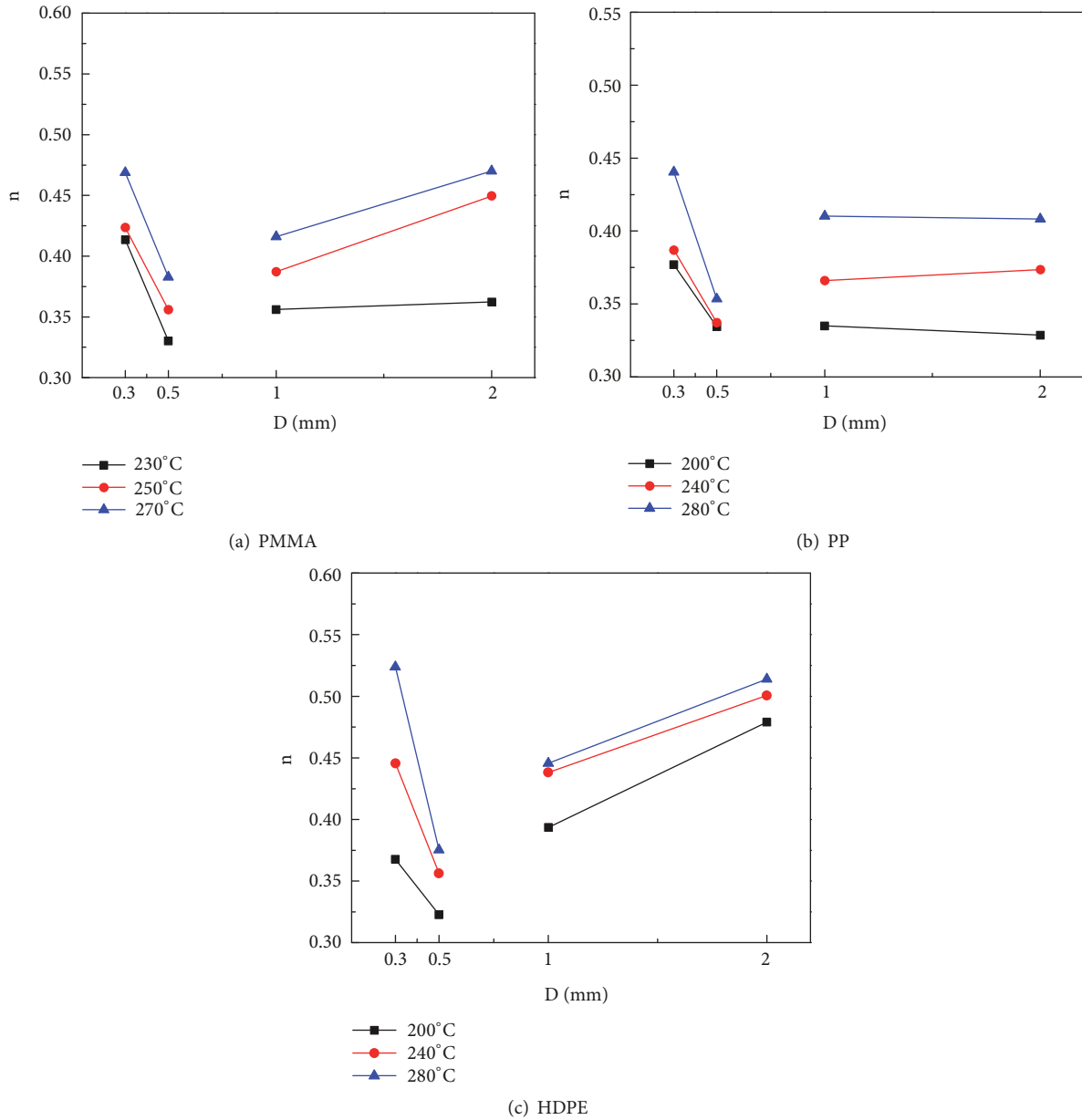


FIGURE 3: Non-Newtonian index of materials at both microscales and macroscales with different temperatures. (a) PMMA; (b) PP; (c) HDPE.

thermal motion. Therefore, it partially reduces the effect of shear rate. The non-Newtonian properties of the melt are attenuated with temperature [15].

The non-Newtonian index decreases with hole diameters of the die at $\phi 0.3$ mm and $\phi 0.5$ mm. It indicates that the larger the hole diameter of the die, the weaker wall sliding effect at the microscale due to the existence of wall slip and that the non-Newtonian properties of the melt increase with the wall shear stress [21].

At the hole diameters of $\phi 1.0$ mm and $\phi 2.0$ mm, the non-Newtonian index of the polymer melt increases or does not change with hole diameters of the die. Reasons are analyzed within the macroscopic scale. On the one hand,

the influence of wall slip is eliminated. On the other hand, with the increased hole diameters of the die, the tensile effect in the convergent flow at the inlet is weakened, and the elastic storage energy is reduced. When the melt flows, the resistance is decreased and the non-Newtonian properties are weakened, resulting in an increase or no change of non-Newtonian index. J. Z. Liang [13] also believes that when the external force conditions are constant, the non-Newtonian index of the melt increases with the diameter of the channel. Therefore, the non-Newtonian index is not only related with melt temperature but also related with feature size. Variations in feature size are bound to cause changes in the melt non-Newtonian index.

TABLE 2: Different material parameters in the size-based viscous flow activation energy (SVAE) model.

| | k_0 | k_1 | k_2 | k_3 | l_0 | l_1 | l_2 | l_3 |
|------|--------|---------|--------|---------|--------|-------|--------|-------|
| PMMA | 310.5 | -820.53 | 834.57 | 241.6 | -0.249 | 0.786 | -0.859 | 0.257 |
| PP | 82.86 | -277.13 | 296.71 | -86.7 | -0.556 | 2.291 | -2.532 | 0.754 |
| HDPE | 178.07 | -475.4 | 477.17 | -138.34 | -0.443 | 0.769 | -0.661 | 0.183 |

TABLE 3: Average error of SVAE model.

| | PMMA | PP | HDPE | Remarks |
|---------------|------|-------|------|---|
| Average error | 7.0% | 15.1% | 7.0% | Compared with the literature [27]/D= ϕ 0.5mm |
| | — — | 11.4% | 3.9% | Compared with the literature [28]/D= ϕ 1mm |
| | — — | — — | 6.8% | Compared with the literature [26]/D= ϕ 1mm |

3.2. Establishment of Model Based on Feature Size

3.2.1. Size-Based Viscous Flow Activation Energy Model. From the above three polymer melt rheology tests, it can be seen that the viscous flow activation energy of the polymer melt is mainly related to the shear rate, the feature size, and the material type. And the viscous flow activation energy has a monotonous decreasing trend with the shear rate. Therefore, considering the influence of the above factors, the size-based viscous flow activation energy model (SVAE model) is developed as follows:

$$E_\eta = \psi A \dot{\gamma}^B \quad (3)$$

where E_η is the viscous flow activation energy of the polymer melt, $\dot{\gamma}$ is shear rate, ψ is model correction factor, and A and B are coefficients related to feature size. According to the testing data of polymer melt, the regression analysis shows that the relationship among the coefficients A and B and feature size D of the die is a cubic polynomial model. Therefore, the viscous flow activation energy model based on feature size is further developed as shown in

$$\begin{aligned} E_\eta &= \psi A \dot{\gamma}^B \\ A &= k_0 + k_1 D + k_2 D^2 + k_3 D^3 \\ B &= l_0 + l_1 D + l_2 D^2 + l_3 D^3 \end{aligned} \quad (4)$$

where $k_0, k_1, k_2, k_3, l_0, l_1, l_2, l_3$ are characteristic parameters of the polymer material, which is related to the type of the material. The parameter values of different materials can be obtained by regression analysis as shown in Table 2.

Figure 4 shows the calculated viscous flow activation energy value of PMMA, PP, and HDPE using the traditional Arrhenius equation, compared with the calculated values of size-based viscous flow activation energy (SVAE) model. It can be seen that the errors of SVAE model of PMMA, PP, and HDPE are 3.23%, 7.6%, and 10.76%, respectively. The calculated viscous flow activation energy value by the conventional equation itself has a certain error, and the feature size has little effect on the viscous flow activation energy for the crystalline polymer material. Therefore, the SVAE model has a larger prediction error for the viscous

flow activation energy value of the crystalline polymer melt than that of the amorphous polymer melt, but it is still acceptable. Therefore, the established SVAE model has a certain precision and reliability for predicting the viscous flow activation energy.

In addition, we use the SVAE model to calculate the viscous flow activation energy values of PMMA, PP, and HDPE as shown in Figure 5. Compared with the data in the literatures [26–28], the average error is calculated as shown in Table 3.

It can be seen that the maximum value of the average error is 15.1%. For the polymer melt, the melt rheology properties have a certain difference under different test conditions, which leads to a large calculation error of the viscous flow activation energy. However, the above error is still within the acceptable range, so the SVAE model has certain accuracy and reliability.

3.2.2. Size-Based Non-Newtonian Exponential Model. From the non-Newtonian index of the polymer melt in Figure 3, it can be seen that the non-Newtonian index value depends on hole diameters of the die, melt temperature, and polymer material type. The non-Newtonian index shows a linear trend with temperature. Considering the influence of the above factors, a size-based non-Newtonian index model (SNNE model) is developed for different materials as follows:

$$n = \xi (kT + b) \quad (5)$$

where n is non-Newtonian index, T is temperature, ξ is the model correction coefficient under different test conditions, and the coefficients k and b are related to the feature size D . The relationship among the coefficients k , b , and D is a cubic polynomial one. Therefore, (6) can be obtained as follows:

$$\begin{aligned} n &= \xi (kT + b) \\ k &= B_0 + B_1 D + B_2 D^2 + B_3 D^3 \\ b &= C_0 + C_1 D + C_2 D^2 + C_3 D^3 \end{aligned} \quad (6)$$

where $B_0, B_1, B_2, B_3, C_0, C_1, C_2, C_3$ are the material parameters, which is related to the material type. The parameter values of different materials can be obtained by regression analysis as shown in Table 4.

TABLE 4: Material parameters in the size-based Non-Newtonian index model (SNNE) model.

| | B_0 | B_1 | B_2 | B_3 | C_0 | C_1 | C_2 | C_3 |
|------|--------|---------|--------|---------|---------|--------|---------|--------|
| PMMA | 0.0069 | -0.0217 | 0.0234 | -0.0068 | -1.0460 | 4.2570 | -4.6360 | 1.3450 |
| PP | 0.0032 | -0.0116 | 0.0134 | -0.0041 | -0.1470 | 1.7740 | -2.1280 | 0.6570 |
| HDPE | 0.0054 | -0.0160 | 0.0162 | -0.0047 | -0.5160 | 2.2190 | -2.0940 | 0.6030 |

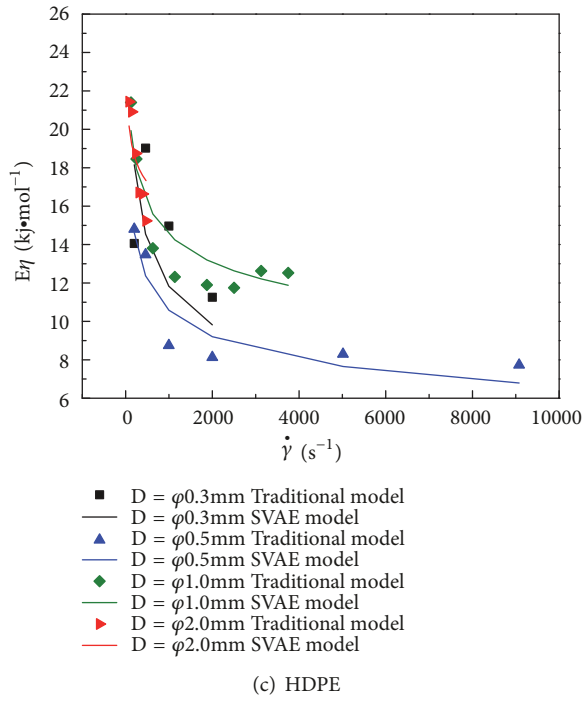
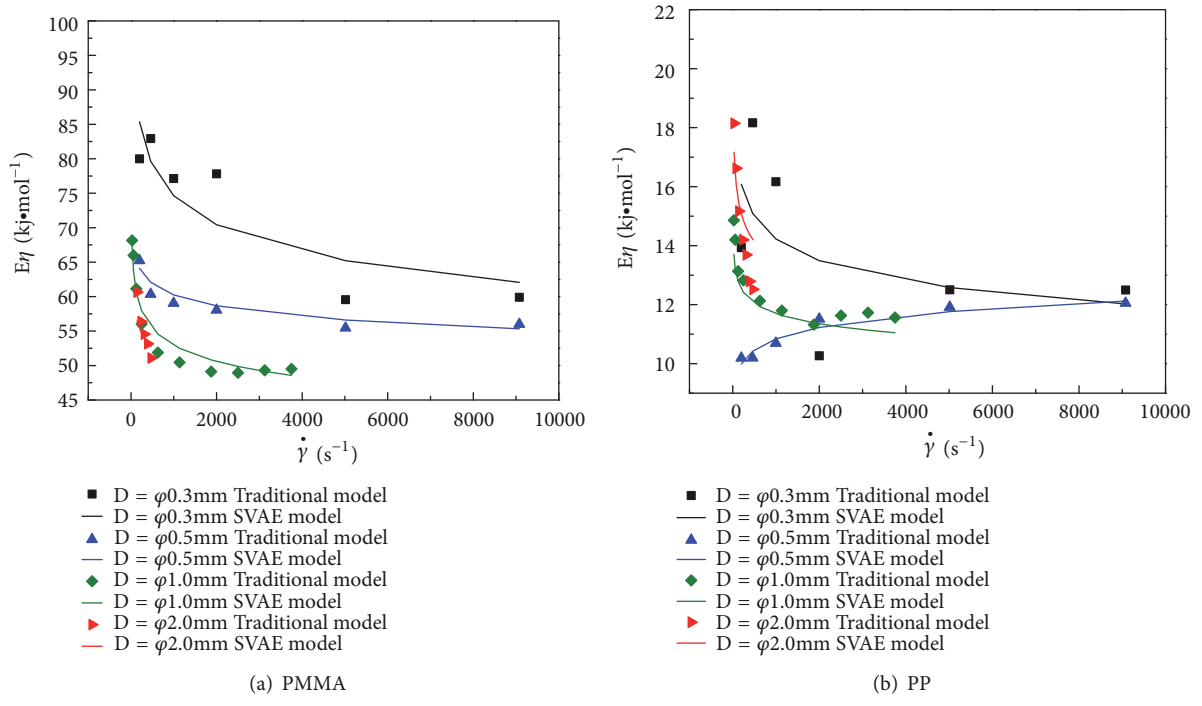


FIGURE 4: Comparison of viscous flow activation energy between conventional equation and SVAE model. (a) PMMA; (b) PP; (c) HDPE.

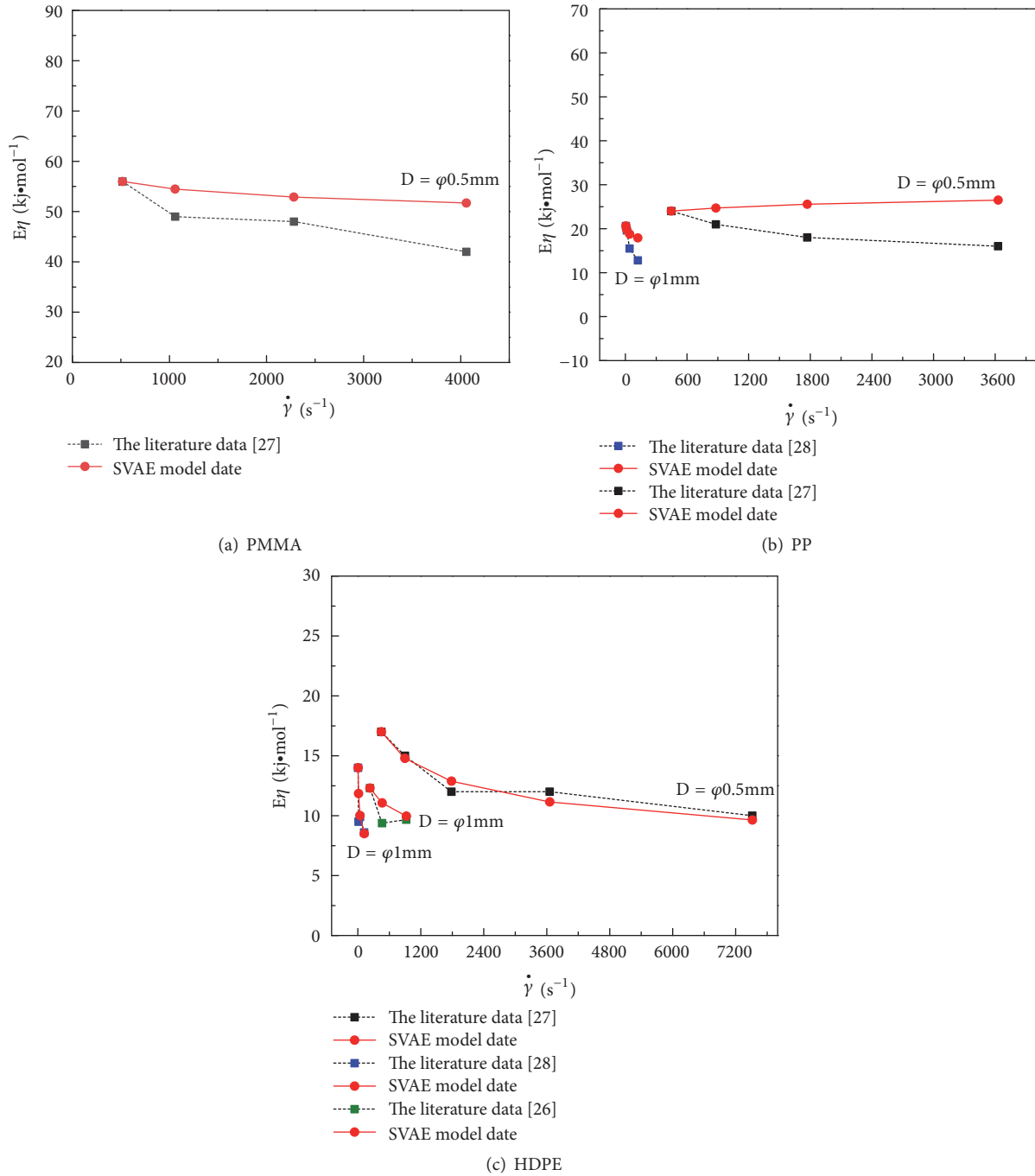


FIGURE 5: Comparison of viscous flow activation energy between SVAE model and the literature data. (a) PMMA; (b) PP; (c) HDPE.

The traditional power law function model shown in (2) and the size-based non-Newtonian index model (SNNE) were used to calculate the non-Newtonian index values of PMMA, PP, and HDPE, respectively. The non-Newtonian index values are shown in Figure 6. The average errors of the SNNE models for the three materials were 2%, 1.7%, and 0.6%, respectively. Therefore, the established SNNE model has high precision and reliability for the prediction of non-Newtonian index values of polymer melts.

In addition, we used the SNNE model to calculate the non-Newtonian index of PMMA, PP, and HDPE from the literatures [26, 27] and compared them with the literature data as shown in Figure 7. It can be seen from Table 5 that the average errors of SNNE model of the non-Newtonian index values are 6%, 5.3%, 0.97%, and 0.81% for PMMA, PP, and HDPE, respectively. Therefore, the SNNE model has a high predicting accuracy for non-Newtonian values of different polymer materials [26, 27].

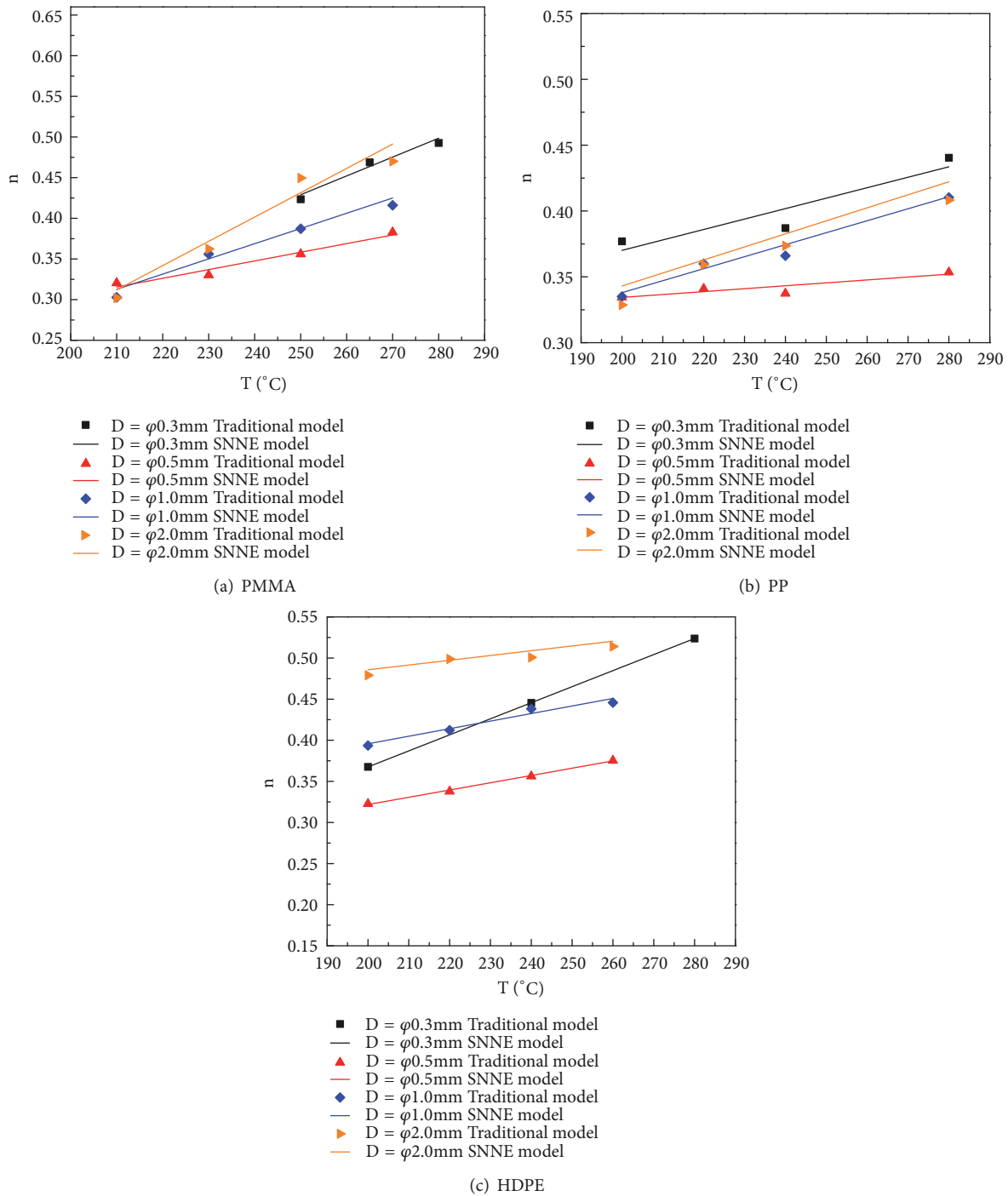


FIGURE 6: Comparison of the non-Newtonian index values of the traditional power law model and the SNNE model. (a) PMMA; (b) PP; (c) HDPE.

4. Conclusion

A series of rheological tests were carried out on the flow properties of PMMA, PP, and HDPE at hole diameters of the die between $\varphi 0.3$ and $\varphi 2$ mm. The viscous flow activation energy model and non-Newtonian index model based on feature size were established.

(1) At the microscopic scale, the viscous flow activation energy of PMMA decreases with the feature size, while the viscous flow activation energy of the crystalline polymer PP and HDPE increases with the die diameter. The viscous flow activation energy difference of all polymer materials is significantly reduced by eliminating the effects of wall slip at the macroscopic scale.

TABLE 5: Average error of SNNE model.

| | PMMA | PP | HDPE | Remarks |
|---------------|-------|-------|-------|--|
| Average error | 6.00% | 5.30% | 0.97% | Compared with the literature [27] / $D = \varphi 0.5\text{mm}$ |
| | --- | --- | 0.81% | Compared with the literature [26] / $D = \varphi 1\text{mm}$ |

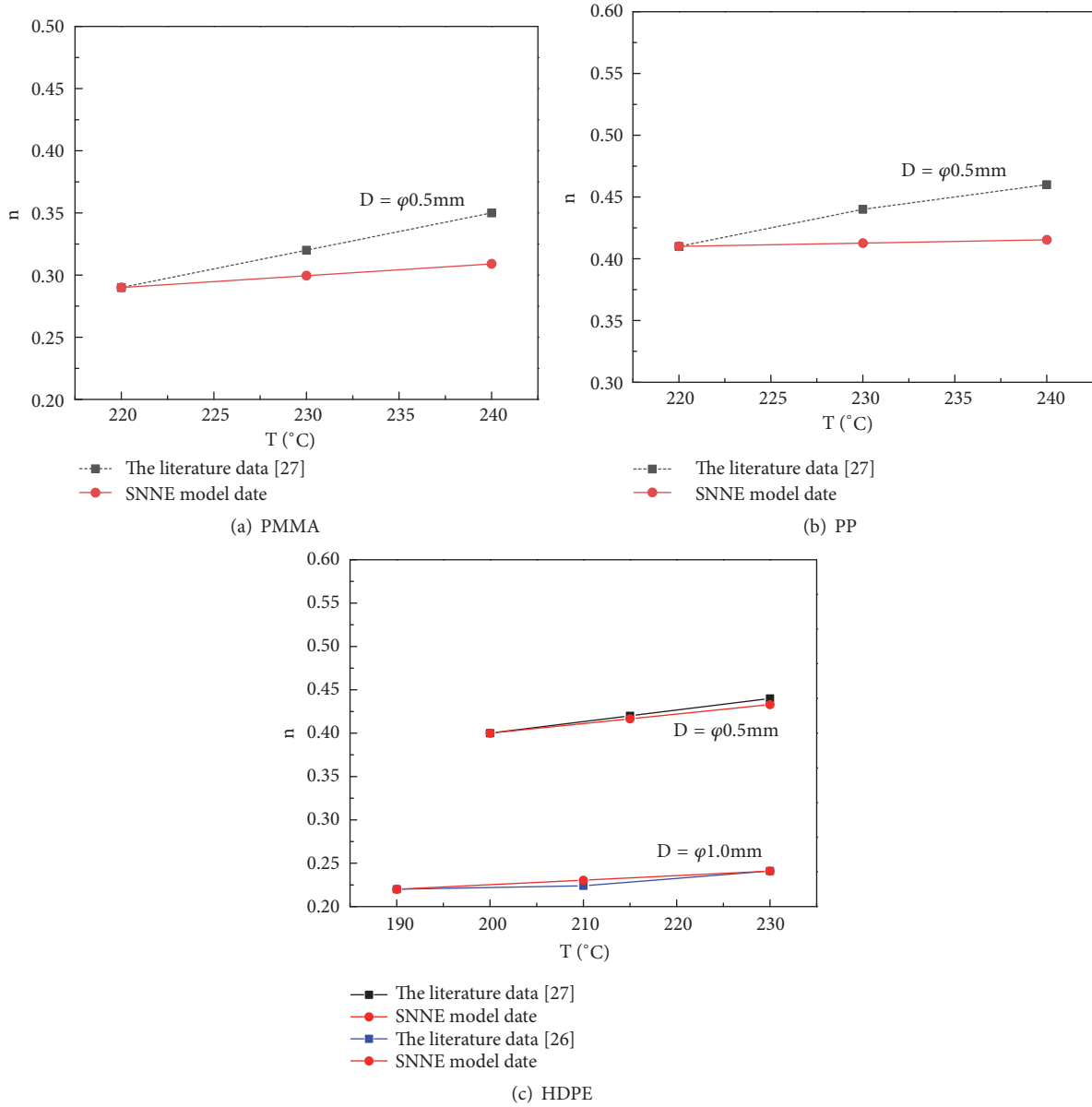


FIGURE 7: Comparison of non-Newtonian index between SNNE model and the literature data. (a) PMMA; (b) PP; (c) HDPE.

(2) The non-Newtonian index of the three polymer materials is decreased with the feature size within the microscopic scale, while it increases or does not change with the feature size within the macroscopic scale.

(3) A viscous flow activation energy model (SVAE model) based on feature size, $E_{\eta} = \psi A \gamma^{\frac{B}{\eta}}$, was established for different polymer materials. The coefficients A and B were

related to the feature size D . The non-Newtonian index model (SNNE model) of the polymer melt based on the feature size, $n = \xi(kT + b)$, was established under different materials and temperatures. The coefficients k and b are related to the feature size D . Finally, the accuracy and effectiveness of the SVAE and the SNNE models are verified by comparing with the traditional model and the literature data.

Through the established SVAE and SNNE models, the viscous flow activation energy and non-Newtonian index values of polymer materials can be calculated conveniently and accurately.

Data Availability

The data used to support the findings of this study are available from the corresponding author upon request.

Conflicts of Interest

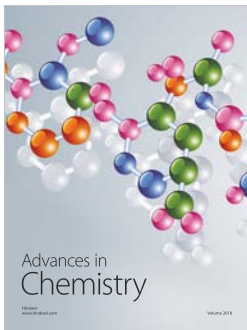
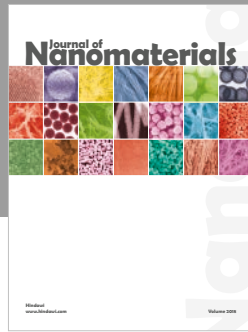
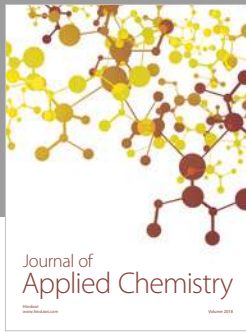
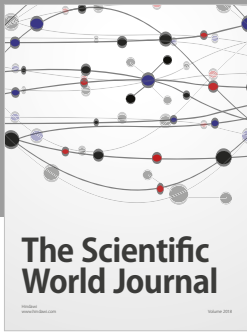
The authors declare that they have no conflicts of interest.

Acknowledgments

The authors gratefully acknowledge research support from the National Natural Science Foundation of China (No. 51675347) and from the Natural Science Foundation of Guangdong Province (No. 2016A030313058).

References

- [1] J. Aho and S. Syrjälä, "On the measurement and modeling of viscosity of polymers at low temperatures," *Polymer Testing*, vol. 27, no. 1, pp. 35–40, 2008.
- [2] J.-Z. Liang, "Characteristics of melt shear viscosity during extrusion of polymers," *Polymer Testing*, vol. 21, no. 3, pp. 307–311, 2002.
- [3] J. Z. Liang and C. Y. Tang, "Studies of melt flow properties during capillary extrusion of polycarbonate," *Journal of Materials Processing Technology*, vol. 63, no. 1-3, pp. 501–504, 1997.
- [4] E. A. Collins and A. P. Metzger, "Polyvinylchloride melt rheology II—the influence of molecular weight on flow activation energy," *Polymer Engineering & Science*, vol. 10, no. 2, pp. 57–65, 1970.
- [5] S. V. Nair, Z. Oommen, and S. Thomas, "Melt elasticity and flow activation energy of nylon 6/polystyrene blends," *Materials Letters*, vol. 57, no. 2, pp. 475–480, 2002.
- [6] H. D. Chandler, "Activation energy and entropy for viscosity of wormlike micelle solutions," *Journal of Colloid and Interface Science*, vol. 409, no. 11, pp. 98–103, 2013.
- [7] F. J. Rubio-Hernández, A. I. Gómez-Merino, R. Delgado-García, and N. M. Pérez-Flor, "An activation energy approach for viscous flow: A complementary tool for the study of microstructural evolutions in sheared suspensions," *Powder Technology*, vol. 308, pp. 318–323, 2017.
- [8] K. Hamad, M. Kaseem, and F. Deri, "Rheological and mechanical characterization of poly(lactic acid)/polypropylene polymer blends," *Journal of Polymer Research*, vol. 18, no. 6, pp. 1799–1806, 2011.
- [9] K. Hamad, M. Kaseem, and F. Deri, "Preparation and characterization of binary and ternary blends with poly(lactic acid), polystyrene, and acrylonitrile-butadiene-styrene," *Journal of Biomaterials and Nanobiotechnology*, vol. 3, no. 3, p. 8, 2012.
- [10] K. Hamad, M. Kaseem, and F. Deri, "Melt rheology of poly(lactic acid)/low density polyethylene polymer blends," *Advances in Chemical Engineering and Science*, vol. 1, no. 4, pp. 208–214, 2011.
- [11] S. Djellali, T. Sadoun, N. Haddaoui, and A. Bergeret, "Viscosity and viscoelasticity measurements of low density polyethylene/poly(lactic acid) blends," *Polymer Bulletin*, vol. 72, no. 5, pp. 1177–1195, 2015.
- [12] M. Kaseem, K. Hamad, F. Deri, and Y. G. Ko, "Effect of wood fibers on the rheological and mechanical properties of polystyrene/wood composites," *Journal of Wood Chemistry and Technology*, vol. 37, no. 4, pp. 251–260, 2017.
- [13] J. Z. Liang, "Effects of extrusion rate, temperature, and die diameter on melt flow properties during capillary flow of low-density-polyethylene," *Journal of Macromolecular Science: Part D - Reviews in Polymer Processing*, vol. 46, no. 3, p. 5, 2007.
- [14] M. Kaseem, K. Hamad, H. W. Yang, Y. H. Lee, F. Deri, and Y. G. Ko, "Melt rheology of poly(vinylidene fluoride) (PVDF)/low density polyethylene (LDPE) blends," *Polymer Science - Series A*, vol. 57, no. 2, pp. 233–238, 2015.
- [15] M.-J. Wang, X.-W. Sun, and Y. Liu, "Experimental study of rheological characteristics of polymer melts under various die diameters," *Journal of Dalian University of Technology*, vol. 50, no. 1, pp. 52–57, 2010.
- [16] X. Bin, "Theoretical and experimental approach of the viscosity of polymer melt under micro-scale effect," *Journal of Mechanical Engineering*, vol. 46, no. 19, p. 125, 2010.
- [17] M. J. Wang, "Micro-scale shear viscosity testing approach and viscosity model of polymer melts," *Journal of Mechanical Engineering*, vol. 48, no. 16, p. 21, 2012.
- [18] L. C. Chi, X. Yu, J. Li, and L. Xu, "Research on melt rheological properties of PP/PET blends," *Plastic Technology*, vol. 41, no. 05, pp. 43–47, 2013.
- [19] C. Z. Wu, "A calculation method of non-Newtonian index of polymer melt," *Synthetic Rubber Industry*, no. 2, pp. 96–100, 1985.
- [20] D. Yao and B. Kim, "Simulation of the filling process in micro channels for polymeric materials," *Journal of Micromechanics and Microengineering*, vol. 12, no. 5, pp. 604–610, 2002.
- [21] Y. Q. Shen, *Study of Rheology Behaviors of Polymer Melt in Micro-Channels [Ph. D. thesis]*, Zhenzhou University, 2010.
- [22] X. W. Sun, *Experimental studies on the rheological characteristics of polymer melts [Ph D. thesis]*, Dalian University of Technology, 2007.
- [23] C. Yang and H. X. Huang, "Rheological Properties of Polymer Melt under condition equivalent to micro injection molding," *Plastic*, vol. 41, no. 05, pp. 60–62, 2012.
- [24] T. Yu, Y. Wu, and T. Jiang, "Effects of ultrasonic field on filling performance of the micro-mold cavity," *Polymer Materials Science & Engineering*, vol. 31, no. 5, pp. 99–104, 2015.
- [25] C. J. Zuo and Y. X. Gu, *Basic Principle And Process of Polymer Material Forming Processing*, Beijing Institute of Technology Press, 2017.
- [26] Q. B. Zhang, Z. Ke, and G. F. Bao, "Study on rheological properties during capillary extrusion of high-grade HDPE pipe," *China Plastics Industry*, vol. 07, pp. 111–113, 2011.
- [27] D. Y. Zhao, Y. F. Jin, M. J. Wang, X. W. Sun, and M. C. Song, "Experimental study on the rheological characteristics of polymer melts under micro scale effect," *Materials Science Forum*, vol. 628, pp. 429–434, 2009.
- [28] L. Li, P. J. Yang, and Z. Zhang, "Study on flow activation energy of PE and PP resins," in *Applied Chemical Industry*, vol. 01, pp. 33–36, 2008.



Hindawi
Submit your manuscripts at
www.hindawi.com

